Global patterns of soil organic carbon distribution in the 20 − 100 cm soil profile for different ecosystems: A global meta-analysis

Haiyan Wang[1,2], Tingyao Cai[1], Xingshuai Tian[1], Zhong Chen[1], Kai He[1], Zihan Wang[1], Haiqing Gong[1], Qi Miao[1], Yingcheng Wang[1], Yiyan Chu[1], Qingsong Zhang[1], Minghao Zhuang[1], Yulong Yin[1,*], Zhenling Cui[1]

[1] State Key Laboratory of Nutrient Use and Management, College of Resources and Environmental Sciences, China Agricultural University, 100193 Beijing, China

[2] Sanya Institute of China Agricultural University, 572025 Sanya, China

[*]**Corresponding author**: Yulong Yin. Email: yinyulong88221@163.com

Manuscript submitted to: Earth System Science Data

Abstract

Determining the distribution of soil organic carbon (SOC) in subsoil (20–100 cm depth) is important with respect to the global C cycle and warming mitigation. However, significant knowledge gaps remain regarding the spatiotemporal dynamics of SOC within this layer. By integrating traditional depth functions with machine learning approaches, we quantified soil β values, which represent the relative rate of decline in SOC density with depth, and provided high-resolution assessments of SOC dynamics across global ecosystems, including cropland, grassland, and forestland. The estimated subsoil SOC densities were 62 Mg ha^{-1} (95% CI: 52-73) for cropland, 70 Mg ha^{-1} (95% CI: 57-83) for grassland, and 97 Mg ha^{-1} (95% CI: 80-117) for forestland. SOC density exhibited a consistent decline with depth, ranging from 30 Mg ha^{-1} to 5 Mg ha^{-1} in cropland, 32 Mg ha^{-1} to 7 Mg ha^{-1} in grassland, and 40 Mg ha^{-1} to 13 Mg ha^{-1} in forestland, across 20 cm depth increments from 20 to 100 cm. The estimated global subsoil SOC stock was 803 Pg C, with cropland, grassland, and forestland contributing 74 Pg C, 181 Pg C, and 547 Pg C, respectively. On average, 57% of this carbon was stored within the top 0-100 cm of the soil profile. This study provides information on the vertical distribution and spatial patterns of SOC density at a 10 km resolution across global ecosystems, providing a scientific basis for future studies pertaining to Earth system models. The dataset is open-access and available at https://doi.org/10.5281/zenodo.15019078 (Wang et al., 2025).

Keyword: Subsoil SOC distribution; Soil profiles; Random Forest; Driving factors; Global ecosystems

1. Introduction

Soil organic carbon (SOC) plays a pivotal role in global carbon cycling, climate change mitigation, reducing greenhouse gas emissions, while simultaneously supporting ecosystem health (Bradford et al., 2016; Lal et al., 2021; Griscom et al., 2017). Subsoil, defined here as the soil layer below 20 cm, contains over half of the global SOC stock (Jobbágy & Jackson, 2000; Poffenbarger et al., 2020; Batjes, 1996). However, the extensive loss of SOC through agricultural practices such as crop production and grazing has substantially contributed to rising atmospheric CO_2 levels (Beillouin et al., 2023; Lal, 2020; Qin et al., 2023). Complex polymeric carbon in subsoil is vulnerable to decomposition under future warming. Specifically, ecological or trophic limitations of SOC biodegradation in deep soil layers can lead to sharp declines in the nutrient supply and biodiversity (Chen et al., 2023). Subsoil is better suited to long-term C sequestration than topsoil. The '4 per 1000' initiative aims to boost SOC storage in agricultural soils by 0.4% annually, offering a potential pathway for mitigate climate change and increase food security (Chabbi et al., 2017). Promoting subsoil carbon sequestration, particularly in agricultural and managed ecosystems, could facilitate the long-term stabilization of fossil-fuel-derived carbon in soils (Button et al., 2022). Despite the importance of subsoil organic carbon dynamics, we were still poorly understood, especially at large scale (Padarian et al., 2022). This is primarily due to the challenges associated with measuring SOC at greater depths, which is difficult, time-consuming and labor-intensive.

Recent studies have focused on SOC allocation and dynamics at varied depths and the subsoil SOC–Climate feedback cycle of terrestrial ecosystems (Luo et al., 2019; Jia et al., 2019; Li et al., 2020). The complexity, uncertainty, and large spatial heterogeneity of SOC stock estimation have limited the ability to accurately quantify the SOC stock distribution (Mishra et al., 2021; Wang et al., 2022a). Currently, three primary methods are commonly used to estimate large-scale SOC stocks: (1) area-weighted averaging based on vegetation inventories and soil survey data (Tang et al., 2018); (2) machine-learning based on remote-sensing, land-use, and edaphic data and climatic factors as covariates (Ding et al., 2016); and (3) depth distribution function-based empirical analysis (Wang et al., 2023). The first approach provides the most accurate measurement of the SOC stock, but is time-consuming and labor intensive and is not practical at the global scale. The latter two do not fully consider the vertical distribution

of the soil profile or the soil properties of various ecosystems. Extrapolating surface SOC measurements from 0–40 cm or 0–50 cm to predict subsoil SOC at greater depths, such as 0–100 cm or 0–200 cm, introduces significant uncertainty, hindering precise estimation of the global subsoil SOC stock (Wang et al., 2023; Ding et al., 2016).

Studies of whole-soil profiles have recorded greater changes in the SOC dynamics of the subsoil under warming (Zosso et al., 2023; Luo et al., 2020; Soong et al., 2021). The amount and quality of C in input soil, such as aboveground litter and root biomass input, could profoundly alter the vertical SOC distribution (Lange et al., 2023; Feng et al., 2022). The β model, in particular, uses simple and flexible functions that capture the relative slope of depth profiles with a single parameter, with the advantage of being able to integrate SOC values from the surface down to a given depth (Jobbágy and Jackson., 2000). The β model was originally applied to vertical root distributions and has been used to fit the steepest reductions with depth (Gale and Grigal, 1987; Jackson et al., 1997). Some researchers have used the global average β of 0.9786 to calculate deep soil SOC stocks (Yang et al., 2011; Deng et al., 2014). However, the different hydrological conditions, soil type, and ground/underground organic matter have limited the ability to resolve the SOC depth distribution with confidence.

In this study, we produced spatially resolved global estimates of the depth distribution and stocks of subsoil SOC using the β model as a depth distribution function-based empirical approach for evaluating cropland, grassland, and forestland ecosystems on a global scale. We collected and analyzed 17,984 observation data from globally distributed soil profiles (0–100 cm) across 14,550 sites to estimate soil β values. We then developed a random forest (RF) model to estimate the spatial variation in grid-level soil β values in the associated ecosystems to resolve the dynamics of the SOC density in different soil layers and subsoil stocks of the global ecosystems.

2. Methods

2.1. Data collection

We conducted peer-reviewed literatures review of studies previously published on SOC stock or SOC content of soil profile between 1980 and 2023 to obtain a database. The Web of Science and China National Knowledge Infrastructure (CNKI) database were searched using the terms “Soil organic carbon” AND “Soil profile” OR “Subsoil” OR “Deep soil”. And the criteria were as follows: (1) The research scope is worldwide. (2)

The study was conducted in the field. (3) The profiles of multiple sites are reported in the same literature, and the profile of each site is considered as an independent study. (4) Profiles with more than three suitable measurements of organic carbon in the first meter were collected from the analysis for there was sufficient detail to characterize the vertical distribution of SOC. (5) The data extracted from included basic site information including location latitude and longitude, soil organic carbon (SOC), total nitrogen (TN), soil bulk density (BD), soil pH and CN ratio, Microbial biomass carbon and nitrogen (MC), Microbial biomass nitrogen (MN), soil clay content, climate conditions (mean annual precipitation (MAP) and mean annual temperature (MAT)). If the soil organic matter (SOM) rather than SOC was reported, the value was converted to SOC by multiplication with a conversion factor of 0.58 (Don et al., 2011). To extract data presented graphically, the digital software GetData Graph Digitizer 2.25 (getdata-graph-digitizer.com) was used. A total of 209 peer-reviewed papers comprising 1,221 soil profiles were included in this dataset, including 758 for cropland, 219 for forestland, and 244 for grassland. Additionally, an expanded dataset was sourced from the WoSIS Soil Profile Database, contributing 7,636 profiles for cropland, 4,534 for forestland, and 4,593 for grassland (Figure 1a). Missing soil and climate factor data from a few sites were either provided by the study authors through direct correspondence, or obtained from the spatial datasets (section 2.2), based on latitude and longitude. These completed data were analyzed to determine the impact of the environment on soil β values and develop a model to predict global grid-level β values, subsequently, soil profiles SOC density, and calculate SOC stocks. Additionally, the soil samples are classified into four major types: sandy soil, loam, clay loam, and clay soil, according to the international soil texture classification standard (Zhao et al., 2022).

2.2 Calculation of soil attributes from literature-derived database

Since the 0–1 m soil profile has different layers in the row data, mass-preserving spline method (R Package 'mpspline2') was used to divide the soil profiles into 5 layers with 20 cm interval. This function implements for continuous down-profile estimates of soil attributes (SOC, TN, Clay, MC, MN, etc.) measured over discrete, often discontinuous depth intervals. In some studies, bulk density data below the 20 cm soil layer were lacking. Notable differences in global SOC stocks estimations were attributed to the values used for soil bulk density. Therefore, we use the database issued by predecessors to generate bulk density data with 0-1m profile at 20 cm interval (Shangguan et al.,

2014). The equation used to calculate SOC density at each research site was the following:

$$SOC\ density = SOC * BD * D * (1 - GC/100)/10 \quad [1]$$

where SOC is the SOC concentration (g kg^{-1}), BD is the soil bulk density (g cm^{-3}), and D is the thickness of the soil layer (at intervals of 20 cm in the first meter), SOC density (Mg C ha^{-1}). GC (>2 mm) is the gravel content (%).

2.3 Calculation of soil β values from literature-derived database

To enhance the comparability of data from different studies, the corresponding soil β values were calculated using Equation 2, which follows the methodology adopted by Yang et al. (2011). The SOC density in the top 0–100 cm was calculated from the initial depth SOC density using Equation 3, which was developed by Jobbágy & Jackson (2000). The equations are as follows:

$$Y = 1 - \beta^{d} \quad [2]$$

$$X_{100} = \frac{1-\beta^{100}}{1-\beta^{d_0}} * X_{d0} \quad [3]$$

where Y represents the cumulative proportion of the SOC density from the soil surface to depth d (cm); β is the relative rate of decrease in the SOC density with soil depth; A lower β indicates a steeper decline with depth. X_{100} denotes the SOC density within the upper 100 cm; d_0 represents the depth of the 0-20 cm soil layer; (cm); and X_{d0} is the SOC density of the top 20 cm soil depth.

2.4 Spatial gridded datasets

The gridded datasets included forestland, grassland, and cropland areas, climate factors and soil properties. Areas of cropland, forestland, and grassland were obtained from Global Agro-Ecological Zones (GAEZ, https://gaez.fao.org/) at a resolution at 0.083° × 0.083°. The MAP and MAT were acquired from the Climatic Research Unit Time Series (CRU TS ver. 4.05; (https://crudata.uea.ac.uk/cru/data/hrg/cru_ts_4.05/cruts.2103051243.v4.05/). The spatial SOC, total N, soil clay contents, and soil pH and gravel content were acquired from the Harmonized World Soil Database ver. 1.2 (https://www.fao.org/soils-portal/data-hub/soil-lassification/worldreference-base/en/). MC and MN data were obtained from this study (Xu et al., 2013). The BD and gravel content (GC) datasets of

the whole soil profile was acquired from Harmonized World Soils Database version 2.0 (HWSD v2.0) (https://gaez.fao.org/pages/hwsd), whose resolution is 1 km. The belowground net primary productivity (BNPP) data were sourced from Xiao et al. (2023). All data were resampled at 0.083° resolution using the "raster" R package (https://rspatial.org/raster).

2.5 Application of RF modeling to predict spatial β values

We reconstruct the relationships among multiple factors, cropland, grassland and forestland soil β values by RF algorithm. The developed RF models were used to predict grid-level soil β values for each ecosystem. Prior to constructing the RF model, the optimal parameter values of m_{try} and *ntrees* were determined through the bootstrap sampling method, which was performed with the "e1071" R package. Predictions of soil β values derived by RF and random-effects regression models were evaluated by 10-fold cross-validation. The dataset was divided into 10 subsets of equal size, of which 70% were used for model fitting and RF procedures, then predicted with the fitted models using the remaining 30% of the data. The performance of RF models was evaluated based on the coefficient of determination (R^2) and root mean square error (RMSE) according to those following equations:

$$R^2 = 1 - \frac{\sum_{p=1}^{q}(y_p - \hat{y}_p)^2}{\sum_{p=1}^{q}(y_p - \bar{y})^2} \quad [4]$$

$$RMSE = \sqrt{\frac{\sum_{p=1}^{q}(y_p - \hat{y}_p)^2}{q}} \quad [5]$$

where y_p represents an observed value (p = 1, 2, 3, …), $\hat{y}_p$ represents the corresponding predicted value (p = 1, 2, 3, …), $\bar{y}$ represents the mean value of observed values, and q represents the total number of observed values.

2.6 Estimating global SOC density and SOC stocks ecosystems across different ecosystems

To reveal the dynamics of SOC with depth, we used the globally predicted β values for cropland, grassland, and forestland ecosystems in Equation 3 to calculate cumulative SOC density at specific depths (e.g., 40, 60, 80, and 100 cm). Based on these cumulative values, the SOC density for each 20 cm interval as calculated by subtracting the cumulative SOC density of the shallower depth from the deeper depth. Subsequently, the total carbon stocks for different ecosystems worldwide were calculated by multiplying the SOC density by the corresponding land area (see Equation 6).

$$SOC\ stocks = SOC\ density * S_{ecosystem} \quad [6]$$

Where $S_{ecosystem}$ is the areas of cropland, grassland or forestland (ha), SOC stocks (Pg C).

2.7 Uncertainty analysis

A Monte Carlo simulation was used to estimate the overall uncertainty in the estimated spatial SOC density. The uncertainty mainly came from be soil β estimation-related parameters and the RF model. Input parameters in the RF model prediction followed independent normal distributions by assuming the grid value as the mean value and its 10 % as the standard deviation (Liu et al., 2024; Xu et al., 2023; Vande et al., 2004). Then, 1,000 random samplings were used to obtain the interval of each grid via Monte Carlo simulations. The sampling value was then used to run the RF model to predict the grid-level soil β with 100 bootstraps to run the RF model. Then we used predicted grid-level soil β to recalculated the distribution of SOC density (SOCD) across different ecosystem. Finally, we calculated the mean along with the 2.5% and 97.5% percentiles to establish the 95% confidence interval of SOC density and SOC stocks.

$$U_i = \frac{CI_i}{x_i} \quad [7]$$

Where x_i is the mean of prediction, CI_i is the confidence interval of x_i, U_i *is the* uncertainty

2.8 Data management and analyses

One-way analysis of variance at $p < 0.05$ was applied to identify significant differences in soil β values using SPSS ver. 20.0 (SPSS, Inc., Chicago, IL, USA) software. We made a database of peer-reviewed publications with Excel 2010 software (Microsoft Corp., Redmond, WA, USA). Weather data analyses were performed using MATLAB R2017a software (MathWorks Inc., Natick, MA, USA). Weather data were analyzed using MATLAB R2017a (MathWorks, Natick, MA, USA). R software (ver. 3.5.1; R Development Core Team, Vienna, Austria) was used to generate graphs. A publicly available map of China was obtained from the Resource and Environment Data Cloud Platform (http://www.resdc.cn). All map-related operations were implemented using ArcGIS 10.2 software (http:/www.esri.com/en-us/arcgis). All algorithms implemented using the random Forest R package in the R software environment (ver. 3.5.1; R Development Core Team, Vienna, Austria).

3. Results

3.1 Soil β values of the three global ecosystems based on field measurements

We analyzed 17,984 globally distributed soil β values (calculated by SOC density and depths) from 14,550 sites, including 5,940 cropland, 4,209 grassland, and 4,401 forestland sites (Figure 1a). This included an additional 8,394 observations for cropland, 4,753 for forestland, and 4,837 for grassland, obtained from the literature and the WoSIS Soil Profile Database. The average soil β values across all observations were 0.9731 for cropland, 0.9772 for grassland, and 0.9790 for forestland (Figure 1b), with significant differences observed among the ecosystems. Soil β values exhibited significant differences among sandy soil, loam, clay loam, and clay soil. Cropland and grassland ecosystems exhibited the highest β values in sandy soil, while forest ecosystems showed the highest β values in clay soil (Figure 1c-d).

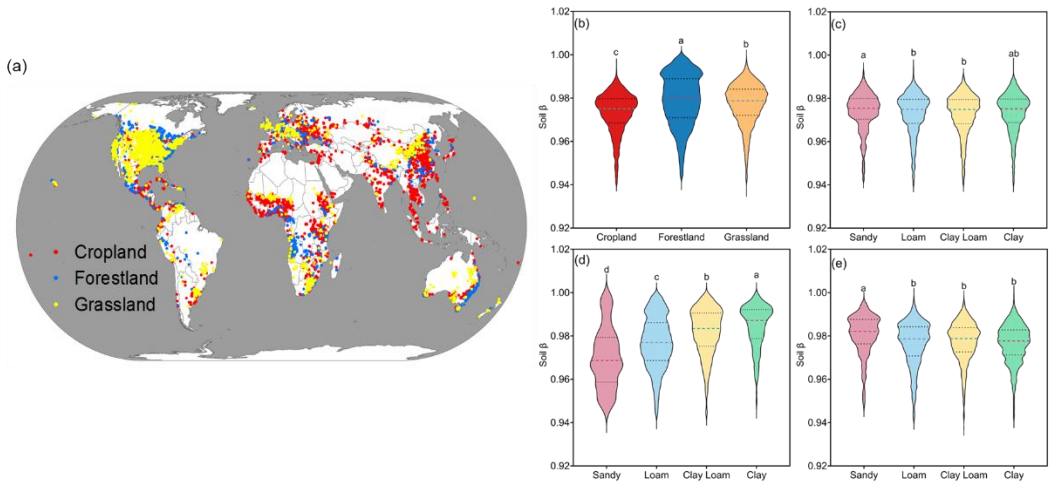

Figure 1. Geographic location of the study sites included in the meta-analysis of the 0–100 cm soil profiles (**a**). Red, yellow, and blue dots represent cropland, grassland, and forestland, respectively. Soil β values of the study sites showing significant differences in different ecosystems with ANOVAR analysis and Duncan's new multiple range test (**b**). **c-e** demonstrate the variations in soil β values across sandy soil, loam, clay loam, and clay for cropland, forestland, and grassland, respectively.

3.2 Impact of soil and climate variables on soil β values

The soil β value is significantly influenced by the combined effects of various climatic, biological, and soil factors. MAT, MAP and BNPP were the most influential driver of β values (Figure S1). Higher MAT promoted increases in soil β values and higher MAP promoted decreases; however, when the MAT was about 20°C and MAP was about

1000 mm, the soil β values growth and decline rate was substantially reduced (Figure 2a and b). BNPP demonstrated a nonlinear relationship: β values decreased with increasing BNPP levels, when BNPP was below 1.5 Mg ha^{-1} yr^{-1} and exceed 2 Mg ha^{-1} yr^{-1}, the soil β values decreased sharply (Figure 2c). The regression between CN, MC, MN, TN, pH and soil β values was parabolic. When CN >10, MC >100 mg/kg, MN >20 mg/kg, TN >3 g/kg and pH <6, the soil β value promoted decreased (Figure 2d, e, f, g and h). β values remained relatively stable across most clay percentages but showed a decrease when clay content exceeded 30% (Figure 2i). Through comparison and analysis, we ultimately selected 9 significant factors (BNPP, pH, Clay, MAT, MAP, TN, MN, MC, CN) for modeling based on their importance and explanatory power (Figure S1).

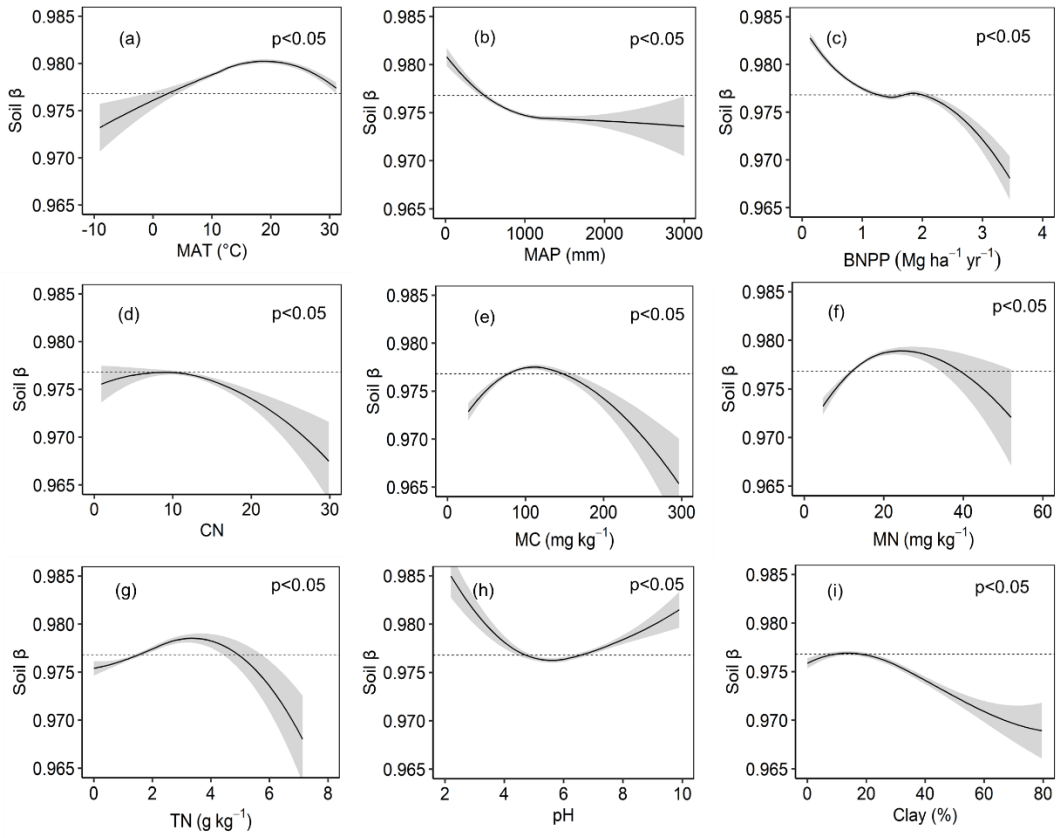

Figure 2. a-i show the variables affecting soil β values. MAT, mean annual temperature; MAP, mean annual precipitation; BNPP, belowground net primary productivity; CN, the ratio of SOC to TN; MC, microbial biomass carbon; MN, microbial biomass nitrogen; TN, soil total nitrogen; pH, soil pH; Clay, clay content. Shaded bands indicate 95% confidence intervals, and the dashed lines represent the average soil β values.

3.3 Performance of the random forest regression model

We developed an RF regression model using machine learning techniques to determine grid-level soil β values on a global scale. The model included 9 significant factors (BNPP, pH, Clay, MAT, MAP, TN, MN, MC, CN), as well as the corresponding high-spatial-resolution raster datasets (Figure S2–S4). The model performed well, with an adjusted coefficient of determination (R^2) of 0.85, 0.86, and 0.90 for cropland, grassland, and forestland, respectively, and the RMSE values are all less than 0.01 (Figure 3a-c). The predictions and measurements of all samples were also distributed close to the 1:1 line. These validations suggest that the trained RF model is capable of capturing and predicting the spatial pattern of the soil β value on a global scale.

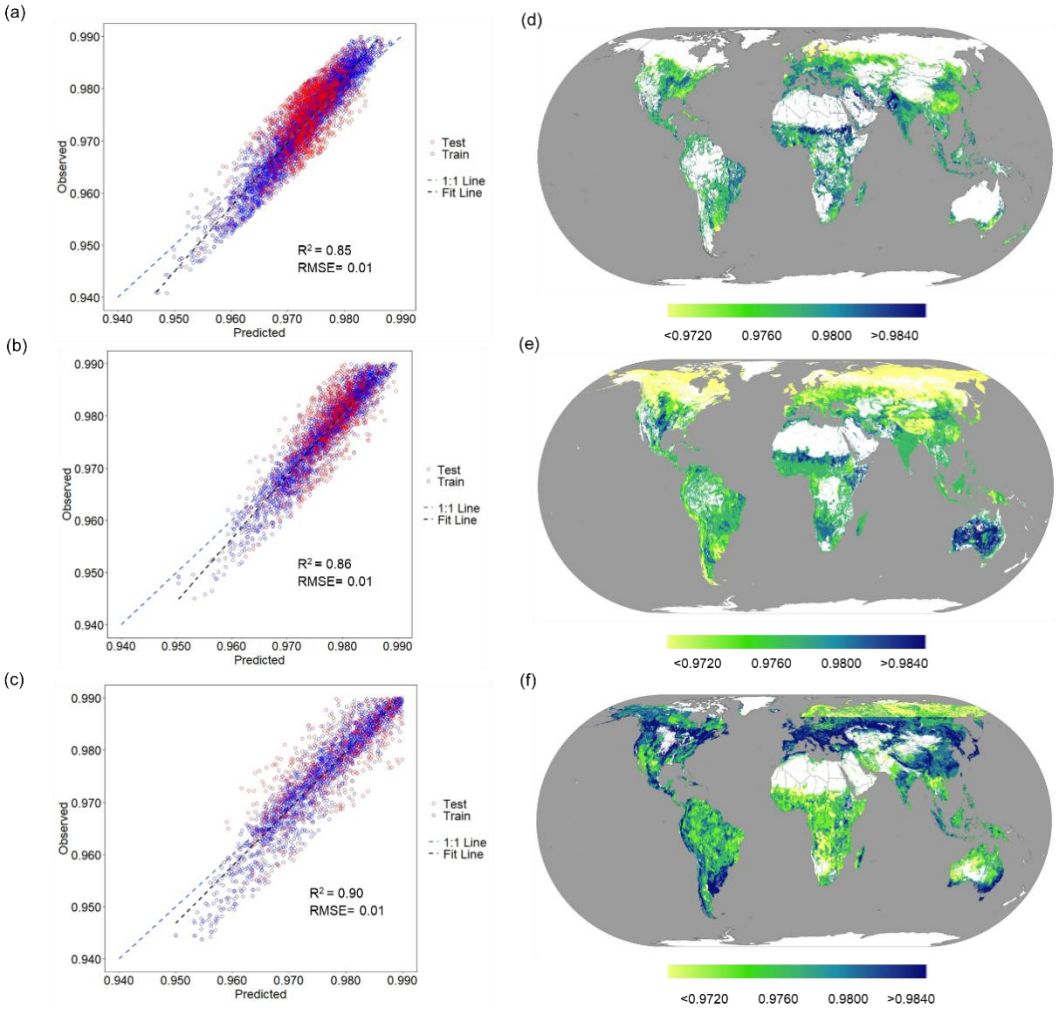

Figure 3. Grid-level maps showing the predicted global soil β values. **a–c** reflect the performance of the random forest model as evaluated by the correlation between the observed and predicted responses of soil β values. **d–f** illustrate the predicted spatial variability of predicted soil β values in cropland, grassland, and forestland, respectively.

3.4 Mapping the global grid-level soil β value

We predicted the global soil β value using the RF model for 4,057,524 integrated grid-level, high-spatial-resolution soil and climate raster datasets (cropland, n = 832,827; forestland, n = 1,695,053; and grassland, n = 1,529,644). The average values were 0.9716 (95% CI: 0.9692-0.9738), 0.9762 (95% CI: 0.9656-0.9831), and 0.9792 (95% CI: 0.9687-0.9877) for cropland, grassland, and forestland, respectively, with CVs of 4.73%, 1.79%, and 1.94% (Figure 3d-f). The spatial distribution of soil β values across cropland, grassland, and forest ecosystems reveals both commonalities and notable differences. High β values are predominantly distributed in tropical and subtropical regions, including parts of South America, Oceania, and sub-Saharan Africa, whereas low β values are mainly concentrated in temperate regions, particularly in northern and western Europe and eastern and northern North America. Notably, the distribution of high β values varies across ecosystems. High β values are primarily observed in sub-Saharan Africa, central North America, and southern Oceania in cropland (Figure 3d). For grassland, mainly concentrated in southeastern South America, southern Africa, and Oceania (Figure 3e). Forestland exhibited the most extensive distribution of high β values, spanning southern South America, central and southern Africa, and Oceania (excluding the central region) (Figure 3f). Cropland exhibits a more confined range of low values, mainly in northwestern Europe, while grassland and forestland display broader areas of low values, particularly across eastern and northern North America. These patterns underscore the geographic variability of soil β values, reflecting the complex interplay between environmental and ecological factors shaping these spatial distributions.

3.5 Spatial variability of the SOC density in subsoil

The estimated values for the global average SOC density of cropland, grassland, and forestland 62 Mg ha^{-1} (95% CI:52-73), 70 Mg ha^{-1} (95% CI:57-83), and 97 Mg ha^{-1} (95% CI:80-117), respectively, for the 20–100 cm layer (Table S1), with considerable spatial variation on the global scale (Figure 4). The larger the soil β value, the more rapidly the SOC density decreased with an increase in soil depth. Spatially, there was geographic variability in the SOC density depending on ecosystems. The higher values exhibited similar spatial patterns in each ecosystems type and were distributed mainly in northern and western Europe and northern and eastern North America.

For cropland, lower SOC density values were predominantly distributed in Eastern and

Southwestern Asia, Sub-Saharan Africa, Southern Africa, Central North America, and Southern Oceania. In contrast, higher SOC density values were mainly concentrated in temperate regions, such as parts of Europe, Northern North America, and some regions in South America (Figure 4a). For grassland, SOC density showed significant spatial variation, with lower values primarily distributed in Eastern and Southwestern Asia, Eastern and Southern South America, and Oceania. In contrast, higher values were concentrated in temperate regions, such as Northern and Western Europe, Northern North America (Figure 4b). For forestland, SOC density displayed clear spatial heterogeneity. Lower values were primarily distributed in Northern South America, Central and Southern Africa, Northeastern Africa, and the Central region of Oceania, areas often characterized by tropical or subtropical climates with rapid organic matter decomposition rates (Figure 4c). In contrast, higher values were predominantly found in temperate and boreal forest regions, including northern and Western Europe, Northern North America, and parts of Eastern Asia. The spatial variation in SOC density at multiple depths (20–40, 40–60, 60–80, and 80–100 cm) was also estimated (Figure S5–S7), which exhibited a decreasing trend with increasing depth.

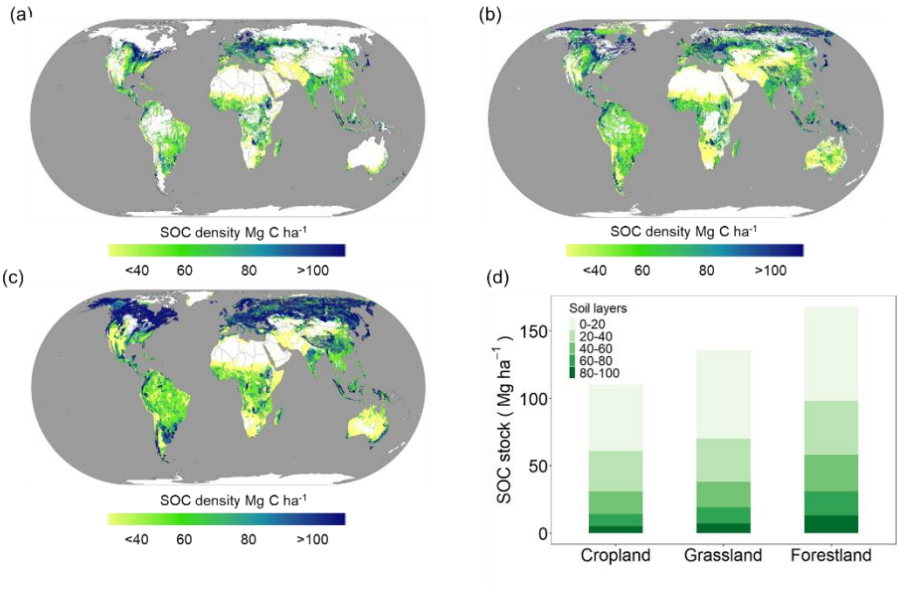

Figure 4. Grid-level maps showing the predicted global subsoil SOC density for the 20–100 cm soil layer. **a–c** represents cropland, grassland, and forestland, respectively. The Plot d shows the SOC density in soil profiles of cropland, grassland, and forestland.

3.6 Uncertainty analysis of subsoil SOC density across ecosystems

Overall, regions with high uncertainty are concentrated in tropical and subtropical areas,

such as sub-Saharan Africa, Southeast Asia, the Amazon region of South America, and parts of Oceania. In contrast, regions with low uncertainty are primarily located in temperate and boreal areas, including northern Europe, Northern North America, and Northern Asia. Among them, forestland exhibits slightly higher SOC density prediction uncertainty (38%) compared to grassland (37%) and cropland (34%) (Figure 5).

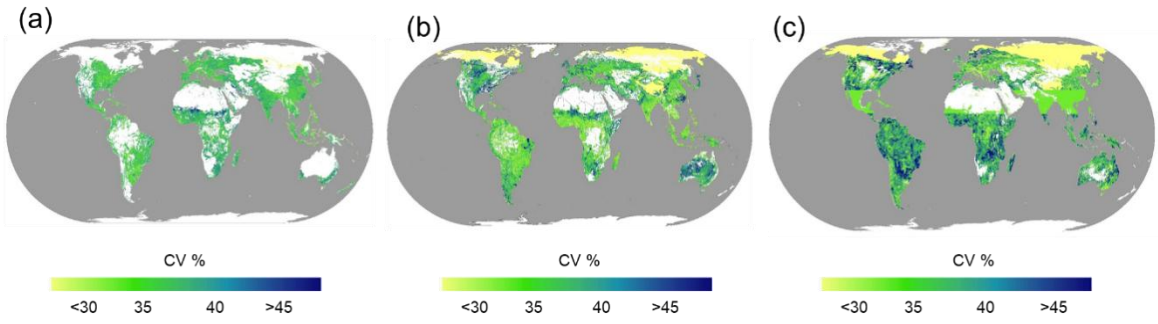

Figure 5. Grid-level maps illustrating the uncertainty of predicted global subsoil SOC density. **a–c** represents cropland, grassland, and forestland, respectively.

4. Discussion

4.1 Comparison of high-resolution SOC dynamics

Global estimations of SOC stock reported in the literature exhibit considerable variation. The estimated SOC stocks for cropland, grassland, and forestland (Table 1) in our study align closely with previous studies (Liu et al., 2021; Conant, 2010; Dixon et al., 1994). The SOC stock of all land in the 0 – 100 cm soil layer was 1418 Pg (95% CI:1276-1577), which was slightly lower than the estimate reported by Sanderman et al. (2017) and Batjes. (1996). However, we believe that our estimation was not underestimated. This discrepancy may be due to the overestimation in (Sanderman et al., 2017), which could be attributed to the suboptimal quality of the training dataset used in their spatial prediction models (R^2=0.54). Earlier assessments (Batjes, 1996) relied on databases that included very few soil profiles from regions such as North America, Oceania, or the northern temperate zones. The subsoil SOC stock of all land was 803 Pg (95% CI:661-962), which was consistent with other research results (Scharlemann et al., 2014; Roland Hiederer. and Köchy., 2011; Zhou et al, 2024). We found that the subsoil contains 57% of total SOC stock in the top 0-1 m soil layer, which is consistent with the percentages cited in previous works (47-55%) (Lal, 2018; Balesdent et al., 2018). Overall, this demonstrates the feasibility and accuracy of our methodology, with the

363 estimations proving to be relatively accurate

364 Similar to the findings of Tao et al. (2023) our study reveals a global SOC density
365 pattern with lower values at low latitudes and higher values at high latitudes. The
366 vertical migration of organic matter is notably more pronounced in northern permafrost
367 regions compared to other areas. For cropland, consistent with the estimates by Wu et
368 al. (2024) the spatial variation in relative SOC density across China shows higher
369 carbon densities in the Northeast Plain, the Yangtze River Basin, and the southeastern
370 hills, while lower values are observed in the arid regions of Northwest China (e.g., the
371 Taklamakan Desert) and the North China Plain. This pattern aligns well with the trends
372 identified in our study. The FAO report "Global Assessment of Grassland Soil Carbon:
373 Current Stocks and Sequestration Potential" aligns with our findings, highlighting high
374 grassland carbon stocks in central China, Northern Russia, Northern Asia, Southeastern
375 South America, and Central North America. However, our study also identifies Europe
376 as having significant carbon stocks. This is mainly because temperate climate,
377 particularly in Northern and Western Europe, is humid and mild, providing favorable
378 conditions for the formation and accumulation of soil organic matter. Unlike croplands
379 and grasslands, forestlands are long-lasting vegetation types, with SOC strongly shaped
380 by local environmental conditions. Zhang et al. (2024) predicted forest SOC stocks
381 across climatic zones and soil types, showing higher stocks in Europe, Russia, and
382 Canada. Mediterranean and temperate regions also have higher SOC than
383 tropical/subtropical regions, consistent with our findings, though their study only
384 considers surface soil.

385 Additionally, we observed higher SOC density in boreal forests and tundra regions,
386 showing spatial variability consistent with the spatial variation in carbon turnover times
387 reported in other study (Li et al., 2023), particularly in northern high-latitude permafrost
388 and tundra areas. This suggests that in low-temperature environments, longer soil
389 carbon turnover times, and lower microbial activity reduce the decomposition rate of
390 soil organic matter, allowing more SOC to accumulate. The highest SOC density and
391 microbial C/N ratios were found at high latitudes in tundra and boreal forests, probably
392 due to the higher levels of organic matter in soils, greater fungal abundance, and lower
393 nutrient availability in cold biomes (Gao et al., 2022).

394 Our estimated SOC density at 111 Mg ha^{-1} (95% CI:101-122) for cropland (Table S1)

was higher than that reported in other study (Liu et al., 2021), and lower than that of tropical cropland (Reichenbach et al., 2023). For forestland, the SOC stock was estimated at 177 Mg ha^{-1} (95% CI: 150–187) for the 0–100 cm soil layer (overall), consistent with the estimate reported by Dixon et al. (1994), but significantly lower than those observed in mangroves and tropical forestland (Atwood et al., 2017; Reichenbach et al., 2023). For grassland, it was 132 Mg ha^{-1} (95% CI:119-145) overall, much higher than that of (Conant et al., 2017). Finally, on a global scale, the SOC density of all land for the 0–100 cm soil layer was estimated at 136 Mg ha^{-1} (95% CI: 123–151), which is significantly higher than the estimate reported by Hiederer & Köchy (2011).

Table 1. Comparisons of the estimated SOC stocks with other studies

	Global area (10^9 ha)	Topsoil (Pg) 0–20/30 (cm)	Subsoil (Pg) 20/30–100 (cm)	Total (Pg) 0–100 (cm)	References
Cropland		58	69	127	Liu et al., 2021
Cropland	1.20	59	74 (95% CI:62-88)	133 (95% CI:121-146)	This study
Forestland	4.10	359	787	1146	Dixon et al., 1994
Forestland	5.64	395	547(95% CI:451-660)	942 (95% CI:846-1055)	This study
Grassland				343	Conant, 2010
Grassland	2.59	161	181 (95% CI:148-215)	342 (95% CI:308-376)	This study
All land		684–724	778–824	1462–1548	Batjes, 1996
All land		699	718	1417	Roland Hiederer. and Köchy., 2011
All land		699	716	1416	Scharlemann et al., 2014
All land		863	961	1824	Sanderman et al., 2017
All				1360	Zhou et al, et al., 2024
All land		615	803 (95% CI:661-962)	1418 (95% CI:1276-1577)	This study

SOC: soil organic carbon, 95% CI: refers to the confidence interval

4.2 Factors affecting soil β values and spatial variation

MAT was the primary drivers of soil β values, exhibiting a significant positive correlation. Specifically, with the increase of MAT, the β value increases, and the decrease of SOC density with depth becomes smaller (Figure 2a). This shows that the higher the β value, the relatively lower the proportion of the SOC storage in the soil surface (consistent with previous research Hartley et al., 2021; Melillo et al., 2017). It is generally accepted that in cold and wet regions, low soil temperatures and/or anaerobic conditions promote the formation of thick organic horizons and peats, resulting in the storage of large amounts of SOC (Garcia-Palacios et al., 2021). Tropical soils have the lowest SOC persistence, while polar/tundra soils and soils dominated by amorphous minerals exhibit the highest SOC abundance and persistence (von Fromm et al., 2024). These differences indicate that soil β values are high in low-latitude regions, such as tropical rainforest areas, and low in high-latitude regions, such as the tundra, showing a spatial distribution pattern. Climate warming may lead to greater SOC losses in surface soils compared to deeper layers, especially in high-latitude SOC-

rich systems (Wang et al., 2022). Experimental results of long-term warming show that soil respiration is sensitive to temperature rise (Xu et al., 2015). It could be driven by the changes in the temperature dependence for microbial process rates (Karhu et al., 2014). As field experiments have shown that warming can modify microbial physiology and resource availability (Poeplau et al., 2017).

We found a significant negative relationship between soil β values and MAP. This suggests that higher precipitation rates are associated with a steeper decrease in SOC density with increasing depth. This is primarily due to the pronounced positive correlation between MAP and the surface SOC density (Liu et al., 2023). In wetter climates where the precipitation exceeds evapotranspiration, there is a strong relationship between mineral-associated SOC concentration and persistence, due to the humid soil environments that favor greater root growth and abundance (Heckman et al., 2023). And, the higher the intensity of precipitation, the more susceptible deep soil carbon is to loss (Sun et al., 2024).

Additionally, BNPP plays a crucial role in the global land carbon cycle and carbon balance, as it is a major source of SOC. The increase in BNPP, along with greater root exudates and changes in microbial activity, may lead to new carbon accumulation (Zheng et al., 2024), which resulted in a decreasing trend of soil β values.

Our results highlight the important role of edaphic properties in explaining variation in soil β values, not just climate and biological factors (Figure S1). The soil CN ratio and soil clay content both exhibited a similar negative correlation with the β value. A higher soil CN ratio may decelerate the decomposition rate of organic matter, thereby facilitating an increase in SOC content in warm and arid regions (Spohn et al., 2023), such that the soil β values would trend downward. Under soil CN ratio > 15, warming significantly enhances the development of root biomass (Bai et al., 2023), this could induce a corresponding SOC accumulation. Clay fraction of the soil can absorb litter-derived C and microbial-derived C, promoting the accumulation of organic carbon (Hicks Pries et al., 2023).

Our results showed that for near-neutral pH soils, the β values tend to be stable. In acidic soils, significant losses of SOC occur because microbial growth is more severely constrained, leading to a reduced efficiency in the decomposition and utilization of organic matter by microorganisms (Malik et al., 2018). Salinization and alkalization

impede plant growth, leading to reduced biomass and lower organic matter input into the soil, causing the soil organic carbon content and organic carbon pool to remain very low (Li et al., 2023). The harsh conditions of saline-alkaline soils hinder microbial survival and activity, reducing their efficiency in decomposing and utilizing organic matter. Soil pH had non-linear relationships with microorganisms, tends to be neutral, and the abundance of microorganisms is higher (Patoine et al., 2022). The combination of these factors explains the higher β values observed under extreme acidic or alkaline conditions. Thus, near-neutral pH soils, may enhance its carbon storage potential by improving microbial growth efficiency and facilitating the channeling of matrix components into biomass synthesis.

The effects of TN, MC, MN on soil β values exhibited the same trend, which initially increased and then decreased. The TN stock in the soil exhibits a significant positive correlation with the SOC stock (Feng et al.,2018), leading to a reduction in the β value in nitrogen-enriched soils. MC had positive relationships with the SOC content across the large spatial scale, because of microbes should be considered not only as a controlling factor of the consumption of SOC, but also as an influencing factor of the production of SOC (Tao et al., 2023). Microbial necromass has been identified as a major contributor to SOC formation across global ecosystems (Wang et al., 2021a). Evidence from China shows that microbial residues contribute a larger proportion of SOC in subsoils than in topsoil (Wen et al., 2023). Therefore, in soil profiles with a high microbial carbon and nitrogen, the soil β value is smaller, indicating a steeper decrease in SOC density with increasing depth.

4.3 Challenges and opportunities: Deep soil SOC sequestration

More and more studies have shown about the necessity to better understand subsoil SOC dynamics. Biotic controls on SOC cycling become weaker as mineral controls predominate with depth (Hicks Pries et al., 2023). The topsoil is rich in carbohydrates and lignin, while the subsoil is rich in protein and lipids, the decrease rate of the ratio of the microbially derived carbon to plant-derived carbon with SOM content was 23%–30% slower in the subsoil than in the topsoil (Huang et al., 2023). Warming stimulates microbial metabolic activity on structurally complex organic carbon, resulting in a larger loss of subsoil polymeric SOC compared to topsoil (Zosso et al., 2023). However, long-term experiments may not be long enough to quantify SOC dynamics in subsoil,

large-scale research methods and machine learning are particularly important and necessary. Based on measured soil profile data and environmental variables, Wang et al. (2021b) employed machine learning methods to assess SOC stocks and spatial distribution of subsoil in frozen soil areas in the third pole region. The investigation of deep soil organic carbon is inherently complex and involves intricate and time-intensive methodologies. This complexity results in a paucity of research data, which consequently introduces considerable uncertainties into model-derived predictions. To avoid under- or overestimation of the SOC stocks of an ecosystem, it is important to consider the subsoil when formulating sequestration policies for the whole soil profile (Button et al., 2022), as the "4 per 1000" approach for the top 30 to 40 cm soil layer provides an incomplete representation of the soil profile (Rumpel et al., 2018). It may be essential to sample the soil deeper (e.g. 0–100 cm) and incorporate deep soils into future manipulations, measurements and models.

In addition, researchers had quantified the contribution of optimizing crop redistribution and improved management, and topsoil carbon sequestration in offsetting anthropogenic greenhouse gas emissions and climate change (Wang et al., 2022b; Rodrigues et al., 2021; Yin et al., 2023), the ability and consequence of subsoil SOC sequestration of crop management remains to be further studied. Conducting global-scale subsoil SOC dynamics studies will fill the knowledge gap to develop appropriate soil C sequestration strategies and policies to help the world cope with climate change and food security (Amelung et al., 2020; Bossio et al., 2020). As such, it is crucial that future research efforts focus on SOC sequestration efficiency with climate change, considering the entire soil profile.

4.4 Strengths and limitations

Our research establishes a scientific foundation for further study of SOC dynamics, sequestration, and emissions reduction across soil profiles, offering significant insights for achieving Sustainable Development Goals (SDGs), notably SDG2 (Zero Hunger), SDG13 (Climate Action), and SDG15 (Life on Land) (https://www.undp.org/sustainable-development-goals). To our knowledge, this is the first study to present global high-resolution maps illustrating the spatial distribution of SOC density within soil profiles, derived from soil β values informed by soil properties and climatic conditions. We observed pronounced variations in SOC density across

ecosystems, with forestland demonstrating the highest densities, followed by grassland and cropland. However, the observed differences in SOC dynamics across these ecosystems were primarily attributed to the dominant biogeochemical properties of the soils (Reichenbach et al., 2023).

In our analysis, we incorporated a broad spectrum of environmental variables, including climatic factors and soil physicochemical properties, to examine subsoil SOC dynamics across different ecosystems. The variability in SOC density decline across soil profiles with depth in most areas underscores the imperative for refined soil management practices. Enhancing carbon sequestration in deeper soil horizons constitutes a promising avenue for future research. For example, increasing plant diversity and crop diversification has reinforced SOC stocks in subsoil, with this benefit amplifying over time (Lange et al., 2023, Xu et al., 2023). Current research has shed light on certain aspects of subsoil SOC sequestration mechanisms and turnover dynamics (Luo et al., 2019; Li et al., 2023). However, implementing targeted policies, such as incorporating organic materials and biochar, remains essential for enhancing the SOC sequestration potential of deeper soils (Button et al., 2022). These strategies could play a critical role in synergistically enhancing soil fertility and mitigating greenhouse gas emissions.

Some important aspects of SOC stocks were not included in this study. For instance, microbial necromass is a key contributor to SOC accumulation (Zhou et al., 2023). Due to difficulties in obtaining management data for grasslands and forestlands, we did not account for potential management-specific factors on soil β value estimations. For example, N fertilizer application, irrigation amount, soil tillage practices, and organic carbon inputs (straw return, crop residues, and litterfall) may influence the vertical movement of SOC. Moreover, organic carbon inputs can alter SOC decomposition rates, particularly in deeper soil layers (Cardinael et al., 2018).

We also acknowledge that soil layers may not always reach 1 meter, especially in mountainous areas. Due to the lack of global soil thickness data, this limitation may lead to overestimation or underestimation of soil carbon storage in some regions. Focusing on 1-meter profiles provides a reasonable approximation of SOC storage across different ecosystems. Although this approach may not fully capture the variation in soil thickness in high mountain areas, it enables us to gain valuable insights into SOC

dynamics within the global carbon cycle. Future studies will incorporate more detailed soil thickness data to improve our understanding of SOC distribution.

5. Data availability

The data of "global patterns of soil organic carbon distribution in the 20–100 cm soil profile for different ecosystems: a global meta-analysis" are available at https://doi.org/10.5281/zenodo.14787023 (Wang et al., 2025). The file named "Rawdata.xlsx" contains data sourced from the literature. The file name is "GE_β.tif", GE represents global ecosystems, which including cropland (CL), grassland (GL), and forestland (FL). "FL_β.tif" represents the spatial distribution of β for forestland at 20-100 cm depth. The file name is "GE_d_SOCD.tif", where SOCD represents soil organic carbon density, d represents soil depth, for example, "FL_20-100_SOCD.tif" represents the spatial distribution of SOCD for forestland at 20-100 cm depth.

6. Conclusion

Accurately quantifying the distribution of soil profile SOC stocks is crucial for C sequestration and mitigation. Herein, machine learning was applied to the β model to estimate SOC stocks in soil profiles at depths of 20–100 cm. The subsoil SOC density values of cropland, grassland, and forestland were estimated to be 62 Mg ha^{-1} (95% CI:52-73), 70 Mg ha^{-1} (95% CI:57-83), and 97 Mg ha^{-1} (95% CI:80-117), respectively, with significant geographic variability across different ecosystems. Additionally, The global subsoil SOC stock was 803 Pg C (95% CI:661-962) (cropland, grassland, and forestland were 74 Pg C (95% CI:62-88), 181 Pg C (95% CI:148-215), and 547 Pg C (95% CI:451-660), in which an average of 57% resided in the top 0–100 cm of the soil profile. This dataset provides a valuable resource for refining existing Earth system models and enhancing prediction accuracy. Furthermore, it offers critical insights into global SOC dynamics and the spatial variability of SOC within entire soil profiles. Our findings also serve as a valuable reference for decision-makers in developing more effective carbon budget management strategies.

Author contributions

The study was completed with cooperation between all authors. ZC and YY conceived and designed the research. HW: conceptualization, investigation, methodology, data curation, visualization, conducted data analysis and wrote original draft. XT:

methodology, data curation, visualization, TC: investigation, data curation, conceptualization, investigation. ZC, KH, ZW, HG, QM, YW, YC, MZ contributed to the scientific discussions. ZC and QZ: conceptualization, supervision, funding acquisition.

Competing interests.

The authors declare that they have no conflict of interest.

Disclaimer. Publisher's note

Copernicus Publications remains neutral with regard to jurisdictional claims in published maps and institutional affiliations.

Acknowledgements.

This work was financially supported by the PhD Scientific Research and Innovation Foundation of Sanya Yazhou Bay Science and Technology City (HSPHDSRF-2022-05-013), and the Hainan Provincial Joint Project of Sanya Yazhou Bay Science and Technology City (2021JJLH0015), and the National Key Research and Development Program of China (2021YFD1900901).

Financial support.

This work was supported by the PhD Scientific Research and Innovation Foundation of Sanya Yazhou Bay Science and Technology City (HSPHDSRF-2022-05-013), and the Hainan Provincial Joint Project of Sanya Yazhou Bay Science and Technology City (2021JJLH0015), and the National Key Research and Development Program of China (2021YFD1900901).

References

Amelung, W., Bossio, D., de Vries, W., Kögel-Knabner, I., Lehmann, J., Amundson, R., Bol, R., Collins, C., Lal, R., Leifeld, J., Minasny, B., Pan, G., Paustian, K., Rumpel, C., Sanderman, J., van Groenigen, J. W., Mooney, S., van Wesemael, B., Wander, M., and Chabbi, A.: Towards a global-scale soil climate mitigation strategy, Nat. Commun., 11, 5427, https://doi.org/10.1038/s41467-020-18887-7, 2020.

Atwood, T. B., Connolly, R. M., Almahasheer, H., Carnell, P. E., Duarte, C. M., Ewers Lewis, C. J., Irigoien, X., Kelleway, J. J., Lavery, P. S., Macreadie, P. I., Serrano, O., Sanders, C. J., Santos, I., Steven, A. D. L., and Lovelock, C. E.: Global patterns in mangrove soil carbon stocks and losses, Nat. Clim. Chang., 7, 523-528, https://doi.org/10.1038/nclimate3326, 2017.

Bai, T., Wang, P., Qiu, Y., Zhang, Y., and Hu, S.: Nitrogen availability mediates soil carbon cycling response to climate warming: A meta-analysis, Glob. Change Biol., 29, 2608-2626, https://doi.org/10.1111/gcb.16627, 2023.

Balesdent, J., Basile-Doelsch, I., Chadoeuf, J., Cornu, S., Derrien, D., Fekiacova, Z., and Hatté, C.: Atmosphere–soil carbon transfer as a function of soil depth, Nat., 559, 599-602, https://doi.org/10.1038/s41586-018-0328-3, 2018.

Batjes, N. H.: Total carbon and nitrogen in the soils of the world, Eur. J. Soil Sci., 47, 151-163, https://doi.org/10.1111/j.1365-2389.1996.tb01386.x, 1996.

Beillouin, D., Corbeels, M., Demenois, J., Berre, D., Boyer, A., Fallot, A., Feder, F., and Cardinael, R.: A global meta-analysis of soil organic carbon in the Anthropocene, Nat. Commun., 14, 3700, https://doi.org/10.1038/s41467-023-39338-z, 2023.

Bossio, D. A., Cook-Patton, S. C., Ellis, P. W., Fargione, J., Sanderman, J., Smith, P., Wood, S., Zomer, R. J., von Unger, M., Emmer, I. M., and Griscom, B. W.: The role of soil carbon in natural climate solutions, Nat. Sustain., 3, 391-398, https://doi.org/10.1038/s41893-020-0491-z, 2020.

Bradford, M. A., Wieder, W. R., Bonan, G. B., Fierer, N., Raymond, P. A., and Crowther, T. W.: Managing uncertainty in soil carbon feedbacks to climate change, Nat. Clim. Chang., 6, 751-758, https://doi.org/10.1038/nclimate3071, 2016.

631 Button, E. S., Pett-Ridge, J., Murphy, D. V., Kuzyakov, Y., Chadwick, D. R., and Jones,
632 D. L.: Deep-C storage: Biological, chemical and physical strategies to enhance
633 carbon stocks in agricultural subsoils, Soil Biol. Biochem., 170, 108697.
634 https://doi.org/10.1016/j.soilbio.2022.108697, 2022.
635 Cardinael, R., Guenet, B., Chevallier, T., Dupraz, C., Cozzi, T., and Chenu, C.: High
636 organic inputs explain shallow and deep SOC storage in a long-term agroforestry
637 system – combining experimental and modeling approaches, Biogeosciences., 15,
638 297-317, https://doi.org/10.5194/bg-15-297-2018, 2018.
639 Chabbi, A., Lehmann, J., Ciais, P., Loescher, H. W., Cotrufo, M. F., Don, A.,
640 SanClements, M., Schipper, L., Six, J., Smith, P., and Rumpel, C.: Aligning
641 agriculture and climate policy, Nat. Clim. Chang., 7, 307-309,
642 https://doi.org/10.1038/nclimate3286, 2017.
643 Chen, J., Luo, Y., and Sinsabaugh, R. L.: Subsoil carbon loss, Nat. Geosci., 16, 284-
644 285, https://doi.org/10.1038/s41561-023-01164-9, 2023.
645 Conant, R. T.. Challenges and opportunities for carbon sequestration in grassland
646 systems: a technical report on grassland management and climate change
647 mitigation, 2010.
648 Conant, R. T., Cerri, C. E. P., Osborne, B. B., and Paustian, K.: Grassland management
649 impacts on soil carbon stocks: a new synthesis, Ecol. Appl., 27, 662-668,
650 https://doi.org/10.1002/eap.1473, 2017.
651 Deng, L., Liu, G. B., and Shangguan, Z. P.: Land-use conversion and changing soil
652 carbon stocks in China's 'Grain-for-Green' Program: a synthesis, Glob. Change
653 Biol., 20, 3544-3556, https://doi.org/10.1111/gcb.12508, 2014.
654 Ding, J., Li, F., Yang, G., Chen, L., Zhang, B., Liu, L., Fang, K., Qin, S., Chen, Y., Peng,
655 Y., Ji, C., He, H., Smith, P., and Yang, Y.: The permafrost carbon inventory on the
656 Tibetan Plateau: a new evaluation using deep sediment cores, Glob. Change
657 Biol., 22, 2688-2701, https://doi.org/10.1111/gcb.13257, 2016.
658 Dixon, R. K., Solomon, A. M., Brown, S., Houghton, R. A., Trexier, M. C., and
659 Wisniewski, J.: Carbon pools and flux of global forest ecosystems, Science., 263,
660 185-190, https://doi.org/10.1126/science.263.5144.185, 1994.

Don, A., Schumacher, J., and Freibauer, A.: Impact of tropical land-use change on soil organic carbon stocks – a meta-analysis, Glob. Change Biol., Glob Change Biol., 17, 1658-1670, https://doi.org/10.1111/j.1365-2486.2010.02336.x, 2011.

Jobbágy E., and Jackson., R. B.: The vertical distribution of soil organic carbon and its relation to climate and veg etation, Ecol. Appl., 10, 423-436, https://doi.org/10.1890/1051-0761, 2000.

Feng, J., He, K., Zhang, Q., Han, M., and Zhu, B.: Changes in plant inputs alter soil carbon and microbial communities in forest ecosystems, Glob. Change Biol.,28, 3426-3440, https://doi.org/10.1111/gcb.16107, 2022.

Feng, J., Wu, J., Zhang, Q., Zhang, D., Li, Q., Long, C., Yang, F., Chen, Q., and Cheng, X.: Stimulation of nitrogen-hydrolyzing enzymes in soil aggregates mitigates nitrogen constraint for carbon sequestration following afforestation in subtropical China, Soil Biol. Biochem., 123, 136-144, https://doi.org/10.1016/j.soilbio.2018.05.013, 2018.

Gale, M. R. and Grigal, D. F.: Vertical root distributions of northern tree species in relation to successional status, Can. J. For. Res., 17(8): 829-834, https://doi.org/10.1139/x87-131, 1987.

Gao, D., Bai, E., Wang, S., Zong, S., Liu, Z., Fan, X., Zhao, C., and Hagedorn, F.: Three-dimensional mapping of carbon, nitrogen, and phosphorus in soil microbial biomass and their stoichiometry at the global scale, Glob Change Biol., 28, 6728-6740, https://doi.org/10.1111/gcb.16374, 2022.

García-Palacios, P., Crowther, T. W., Dacal, M., Hartley, I. P., Reinsch, S., Rinnan, R., Rousk, J., Hoogen, J., Ye, J. S., and Bradford, M. A.: Evidence for large microbial-mediated losses of soil carbon under anthropogenic warming, Nat. Rev. Earth Environ., 2(7), 507-517, https://doi.org/10.1038/s43017-021-00178-4, 2021.

Georgiou, K., Jackson, R. B., Vindušková, O., Abramoff, R. Z., Ahlström, A., Feng, W., Harden, J. W., Pellegrini, A. F. A., Polley, H. W., Soong, J. L., Riley, W. J., and Torn, M. S.: Global stocks and capacity of mineral-associated soil organic carbon, Nat. Commun., 13, 3797, https://doi.org/10.1038/s41467-022-31540-9, 2022.

690 Griscom, B. W., Adams, J., Ellis, P. W., Houghton, R. A., Lomax, G., Miteva, D. A.,
691 Schlesinger, W. H., Shoch, D., Siikamaki, J. V., Smith, P., Woodbury, P., Zganjar,
692 C., Blackman, A., Campari, J., Conant, R. T., Delgado, C., Elias, P., Gopalakrishna,
693 T., Hamsik, M. R., Herrero, M., Kiesecker, J., Landis, E., Laestadius, L., Leavitt,
694 S. M., Minnemeyer, S., Polasky, S., Potapov, P., Putz, F. E., Sanderman, J., Silvius,
695 M., Wollenberg, E., and Fargione, J.: Natural climate solutions, Proc. Natl. Acad.
696 Sci. U. S. A., 114, 11645-11650, https://doi.org/10.1073/pnas.1710465114, 2017.
697 Hartley, I. P., Hill, T. C., Chadburn, S. E., and Hugelius, G.: Temperature effects on
698 carbon storage are controlled by soil stabilisation capacities, Nat. Commun., 12,
699 6713, https://doi.org/10.1038/s41467-021-27101-1, 2021.
700 Heckman, K. A., Possinger, A. R., Badgley, B. D., Bowman, M. M., Gallo, A. C., Hatten,
701 J. A., Nave, L. E., SanClements, M. D., Swanston, C. W., Weiglein, T. L., Wieder,
702 W. R., and Strahm, B. D.: Moisture-driven divergence in mineral-associated soil
703 carbon persistence, Proc. Natl. Acad. Sci. U. S. A., 120, e2210044120,
704 https://doi.org/doi:10.1073/pnas.2210044120, 2023.
705 Hicks Pries, C. E., Ryals, R., Zhu, B., Min, K., Cooper, A., Goldsmith, S., Pett-Ridge,
706 J., Torn, M., and Berhe, A. A.: The deep soil organic carbon response to global
707 change, Annu. Rev. Ecol. Evol. Syst., 54, 375-401,
708 https://doi.org/10.1146/annurev-ecolsys-102320-085332, 2023.
709 Huang, W., Kuzyakov, Y., Niu, S., Luo, Y., Sun, B., Zhang, J., and Liang, Y.: Drivers of
710 microbially and plant-derived carbon in topsoil and subsoil, Glob. Change Biol.,
711 29, 6188-6200, https://doi.org/10.1111/gcb.16951, 2023.
712 Jackson, R. B., Mooney, H. A., and Schulze, E. D.: A global budget for fine root biomass,
713 surface area, and nutrient contents, Proc. Natl. Acad. Sci. U. S. A., 94, 7362-7366,
714 https://doi.org/10.1073/pnas.94.14.73, 1997.
715 Jia, J., Cao, Z., Liu, C., Zhang, Z., Lin, L., Wang, Y., Haghipour, N., Wacker, L., Bao,
716 H., Dittmar, T., Simpson, M. J., Yang, H., Crowther, T. W., Eglinton, T. I., He, J.
717 S., and Feng, X.: Climate warming alters subsoil but not topsoil carbon dynamics
718 in alpine grassland, Glob. Change Biol.,25, 4383-4393,
719 https://doi.org/10.1111/gcb.14823, 2019.

720 Karhu, K., Auffret, M. D., Dungait, J. A., Hopkins, D. W., Prosser, J. I., Singh, B. K.,
721 Subke, J. A., Wookey, P. A., Ågren, G. I., Sebastia, M. T., Gouriveau. F., Bergkvist,
722 G., Meir, P., Nottingham, A. T., Salinas, N., and Hartley, I. P.: Temperature
723 sensitivity of soil respiration rates enhanced by microbial community response,
724 Nature, 513(7516), 81-84, https://doi.org/10.1038/nature13604, 2014.
725 Lal, R.: Digging deeper: A holistic perspective of factors affecting soil organic carbon
726 sequestration in agroecosystems, Glob Change Biol., 24, 3285-3301.
727 https://doi.org/10.1111/gcb.14054, 2018.
728 Lal, R.: Managing soils for negative feedback to climate change and positive impact on
729 food and nutritional security, Soil Sci. Plant Nutr., 66, 1-9,
730 https://doi.org/10.1080/00380768.2020.1718548, 2020.
731 Lal, R., Monger, C., Nave, L., and Smith, P.: The role of soil in regulation of climate,
732 Philos. Trans. R. Soc. Lond. B. Biol. Sci., 376, 20210084,
733 https://doi.org/10.1098/rstb.2021.0084, 2021.
734 Lange, M., Eisenhauer, N., Chen, H., and Gleixner, G.: Increased soil carbon storage
735 through plant diversity strengthens with time and extends into the subsoil, Glob.
736 Change Biol., 29, 2627-2639, https://doi.org/10.1111/gcb.16641, 2023.
737 Li, J. Q., Pei, J. M., Pendall, E., Reich, P. B., Noh, N. J., Li, B., Fang, C. M., and Nie,
738 M.: Spatial heterogeneity and environmental predictors of permafrost region soil
739 organic carbon stocks, Sci. Adv., 7, eaaz5326,
740 https://doi.org/10.1002/advs.202001242, 2021.
741 Liu, Y., Ge, T., van Groenigen, K. J., Yang, Y., Wang, P., Cheng, K., Zhu, Z., Wang,
742 J.,Li, Y., Guggenberger, G., Sardans, J., Penuelas, J., Wu, J., and Kuzyakov, Y.:
743 Rice paddy soils are a quantitatively important carbon store according to a global
744 synthesis, Commun. Earth Environ., 2, 154, https://doi.org/10.1038/s43247-021-
745 00229-0, 2021.
746 Liu, Y., Zhuang, M., Liang, X., Lam, S. K., Chen, D., Malik, A., Li, M., Lenzen, M.,
747 Zhang, L., Zhang, R., Zhang, L., and Hao, Y.: Localized nitrogen management
748 strategies can halve fertilizer use in Chinese staple crop production, Nat. Food,
749 https://doi.org/10.1038/s43016-024-01057-z, 2024.

Liu, Z., Zhou, Q., Ma, Q., Kuang, W., Daryanto, S., Wang, L., Wu, J., Liu, B., Zhu, J., Cao, C., Li, X., Kou, Z., Shou, W., Qian, J., Liu, M., Xin, Z., Cui, X., and Liang, W.: Scale effect of climate factors on soil organic carbon stock in natural grasslands of northern China, Ecol. Indic., 146, 109757, https://doi.org/10.1016/j.ecolind.2022.109757, 2023.

Li, J., Ding, J., Yang, S., Zhao, L., Li, J., Huo, H., Wang, M., Tan, J., Cao, Y., Ren, S., Liu, Y., and Wang, T.: Depth-dependent driver of global soil carbon turnover times, Soil Biol. Biochem., 185, 109149, https://doi.org/10.1016/j.soilbio.2023.109149, 2023.

Li, S., Zhao, L., Wang, C., Huang, H., and Zhuang, M.: Synergistic improvement of carbon sequestration and crop yield by organic material addition in saline soil: A global meta-analysis, Sci. Total Environ., 891, 164530, https://doi.org/10.1016/j.scitotenv.2023.164530, 2023.

Luo, Z., Wang, G., and Wang, E.: Global subsoil organic carbon turnover times dominantly controlled by soil properties rather than climate, Nat. Commun., 10, 3688, https://doi.org/10.1038/s41467-019-11597-9, 2019.

Luo, Z., Luo, Y., Wang, G., Xia, J., and Peng, C.: Warming-induced global soil carbon loss attenuated by downward carbon movement, Glob Change Biol., 26, 7242-7254, https://doi.org/10.1111/gcb.15370, 2020.

Malik, A. A., Puissant, J., Buckeridge, K. M., Goodall, T., Jehmlich, N., Chowdhury, S., Gweon, H. S., Peyton, J. M., Mason, K. E., van Agtmaal, M., Blaud, A., Clark, I. M., Whitaker, J., Pywell, R. F., Ostle, N., Gleixner, G., and Griffiths, R. I.: Land use driven change in soil pH affects microbial carbon cycling processes, Nat. Commun., 9, 3591, https://doi.org/10.1038/s41467-018-05980-1, 2018.

Melillo, J. M., Frey, S. D., DeAngelis, K. M., Werner, W. J., Bernard, M. J., Bowles, F. P., Pold, G., Knorr, M. A., and Grandy, A. S.: Long-term pattern and magnitude of soil carbon feedback to the climate system in a warming world, Science, 358(6359), 101-105, https://doi.org/10.1126/science.aan287, 2017.

Mishra, U., Hugelius, G., Shelef, E., Yang, Y. H., Strauss, J., Lupachev, A., Harden, J. W., Jastrow, J. D., L., P. C., Riley, W. J., Schuur, E. A. G., Matamala, R., Siewert,

780 M., Nave, L. E., Koven, C. D., Fuchs, M., Palmtag, J., Kuhry, P., Treat, C. C., and
781 Zubrzycki, S.: Spatial heterogeneity and environmental predictors of permafrost
782 region soil organic carbon stocks, Sci. Adv., 7, 1-12,
783 https://doi.org/10.1126/sciadv.aaz5236, 2021.
784 Padarian, J., Minasny, B., McBratney, A., and Smith, P.: Soil carbon sequestration
785 potential in global croplands, PeerJ., 10, e13740,
786 https://doi.org/10.7717/peerj.13740, 2022.
787 Patoine, G., Eisenhauer, N., Cesarz, S., Phillips, H. R. P., Xu, X., Zhang, L., and Guerra,
788 C. A.: Drivers and trends of global soil microbial carbon over two decades, Nat.
789 Commun., 13, 4195, https://doi.org/10.1038/s41467-022-31833-z, 2022.
790 Poeplau, C., Kätterer, T., Leblans, N. I., and Sigurdsson, B. D.: Sensitivity of soil carbon
791 fractions and their specific stabilization mechanisms to extreme soil warming in a
792 subarctic grassland, Global Change Biology, 23(3), 1316-1327,
793 https://doi.org/10.1111/gcb.13491, 2017.
794 Poffenbarger, H. J., Olk, D. C., Cambardella, C., Kersey, J., Liebman, M., Mallarino,
795 A., Six, J., and Castellano, M. J.: Whole-profile soil organic matter content,
796 composition, and stability under cropping systems that differ in belowground
797 inputs, Agric. Ecosyst. Environ., 291 106810,
798 https://doi.org/10.1016/j.agee.2019.106810, 2020.
799 Qin, S., Yuan, H., Hu, C., Li, X., Wang, Y., Zhang, Y., Dong, W., Clough, T., Luo, J.,
800 Zhou, S., Wrage-Mönnig, N., Ma, L., and Oenema, O.: Anthropogenic N input
801 increases global warming potential by awakening the “sleeping” ancient C in deep
802 critical zones, Sci. Adv., 9, 1-8, https://doi.org/doi:10.1126/sciadv.add0041, 2023.
803 Reichenbach, M., Fiener, P., Hoyt, A., Trumbore, S., Six, J., and Doetterl, S.: Soil
804 carbon stocks in stable tropical landforms are dominated by geochemical controls
805 and not by land use, Glob. Change Biol., 29, 2591-2607,
806 https://doi.org/10.1111/gcb.16622, 2023.
807 Rodrigues, L., Hardy, B., Huyghebeart, B., Fohrafellner, J., Fornara, D., Barančíková,
808 G., Bárcena, T. G., De Boever, M., Di Bene, C., Feizienė, D., Kätterer, T., Laszlo,
809 P., O’Sullivan, L., Seitz, D., and Leifeld, J.: Achievable agricultural soil carbon

sequestration across Europe from country-specific estimates, Glob. Change Biol., 27, 6363-6380, https://doi.org/10.1111/gcb.15897, 2021.

Roland Hiederer. and Köchy., M.: Global Soil Organic Carbon Estimates and the Harmonized World Soil Database, European Union., https://doi.org/10.2788/13267, 2011.

Sanderman, J., Hengl, T., and Fiske, G. J.: Soil carbon debt of 12,000 years of human land use, Proc. Natl. Acad. Sci. U. S. A., 114, 9575-9580, https://doi.org/10.1073/pnas.1706103114, 2017.

Scharlemann, J. P. W., Tanner, E. V. J., Hiederer, R., and Kapos, V.: Global soil carbon: understanding and managing the largest terrestrial carbon pool, Carbon Manag., 5, 81-91, https://doi.org/10.4155/cmt.13.77, 2014.

Sun, F., Fan, L., Deng, G., Kuzyakov, Y., Zhang, Y., Wang, J., Li, Y., Wang, F., Li, Z., Tariq, A., Sardans, J., Penuelas, J., Wang, and M., Peng, C.: Responses of tropical forest soil organic matter pools to shifts in precipitation patterns, Soil Biol. Biochem., 197, 109530, https://doi.org/10.1016/j.soilbio.2024.109530, 2024.

Soong, J. L., Castanha, C., Hicks Pries, C. E., Ofiti, N., Porras, R. C., Riley, W. J., Schmidt, M. W. I., and Torn, M. S.: Five years of whole-soil warming led to loss of subsoil carbon stocks and increased CO_2 efflux, Sci. Adv., 7(21), doi: 10.1126/sciadv.abd1343, 2021.

Spohn, M., Bagchi, S., Biederman, L. A., Borer, E. T., Bråthen, K. A., Bugalho, M. N., Caldeira, M. C., Catford, J. A., Collins, S. L., Eisenhauer, N., Hagenah, N., Haider, S., Hautier, Y., Knops, J. M. H., Koerner, S. E., Laanisto, L., Lekberg, Y., Martina, J. P., Martinson, H., McCulley, R. L., Peri, P. L., Macek, P., Power, S. A., Risch, A. C., Roscher, C., Seabloom, E. W., Stevens, C., Veen, G. F., Virtanen, R., and Yahdjian, L.: The positive effect of plant diversity on soil carbon depends on climate, Nat. Commun.,14, 6624, https://doi.org/10.1038/s41467-023-42340-0, 2023.

Tang, X., Zhao, X., Bai, Y., Tang, Z., Wang, W., Zhao, Y., Wan, H., Xie, Z., Shi, X., Wu, B., Wang, G., Yan, J., Ma, K., Du, S., Li, S., Han, S., Ma, Y., Hu, H., He, N., Yang, Y., Han, W., He, H., Yu, G., Fang, J., and Zhou, G.: Carbon pools in China's

terrestrial ecosystems: New estimates based on an intensive field survey, Proc. Natl. Acad. Sci. U. S. A., 115, 4021-4026, https://doi.org/10.1073/pnas.1700291115, 2018.

Tao, F., Huang, Y., Hungate, B. A., Manzoni, S., Frey, S. D., Schmidt, M. W. I., Reichstein, M., Carvalhais, N., Ciais, P., Jiang, L., Lehmann, J., Wang, Y. P., Houlton, B. Z., Ahrens, B., Mishra, U., Hugelius, G., Hocking, T. D., Lu, X., Shi, Z., Viatkin, K., Vargas, R., Yigini, Y., Omuto, C., Malik, A. A., Peralta, G., Cuevas-Corona, R., Di Paolo, L. E., Luotto, I., Liao, C., Liang, Y. S., Saynes, V. S., Huang, X., and Luo, Y.: Microbial carbon use efficiency promotes global soil carbon storage, Nature., 618, 981-985, https://doi.org/10.1038/s41586-023-06042-3, 2023.

Wang, C., Qu, L., Yang, L., Liu, D., Morrissey, E., Miao, R., Liu, Z., Wang, Q., Fang, Y., and Bai, E.: Large-scale importance of microbial carbon use efficiency and necromass to soil organic carbon, Glob. Change Biol., 27, 2039-2048, https://doi.org/10.1111/gcb.15550, 2021a.

Wang, D., Wu, T., Zhao, L., Mu, C., Li, R., Wei, X., Hu, G., Zou, D., Zhu, X., Chen, J., Hao, J., Ni, J., Li, X., Ma, W., Wen, A., Shang, C., La, Y., Ma, X., and Wu, X.: A 1 km resolution soil organic carbon dataset for frozen ground in the Third Pole, Earth Syst. Sci. Data., 13, 3453-3465, https://doi.org/10.5194/essd-13-3453-2021b.

Wang, J., Wei, X., Jia, X., Huang, M., Liu, Z., Yao, Y., and Shao, M.: An empirical approach to predict regional organic carbon in deep soils, Sci. China Earth Sci., 66, 583-593, https://doi.org/10.1007/s11430-022-1032-2, 2023.

Wang, M., Guo, X., Zhang, S., Xiao, L., Mishra, U., Yang, Y., Zhu, B., Wang, G., Mao, X., Qian, T., Jiang, T., Shi, Z., and Luo, Z.: Global soil profiles indicate depth-dependent soil carbon losses under a warmer climate, Nat. Commun., 13, 5514, https://doi.org/10.1038/s41467-022-33278-w, 2022a.

Wang, Z., Yin, Y., Wang, Y., Tian, X., Ying, H., Zhang, Q., Xue, Y., Oenema, O., Li, S., Zhou, F., Du, M., Ma, L., Batchelor, W. D., Zhang, F., and Cui, Z.: Integrating crop redistribution and improved management towards meeting China’s food demand

with lower environmental costs, Nat Food., 3, 1031-1039, https://doi.org/10.1038/s43016-022-00646-0, 2022b.

Wang, H., Cai, T., Tian, X., Chen, Z., He, K., Wang, Z., Gong, H., Miao, Q., Wang, Y., Chu, Y., Zhang, Q., Zhuang, M., Yin, Y., and Cui, Z.: Global patterns of soil organic carbon distribution in the 20–100 cm soil profile for different ecosystems: A global meta-analysis [Dataset], Zenodo. https://doi.org/10.5281/zenodo.15019078, 2025.

Wen, S., Chen, J., Yang, Z., Deng, L., Feng, J., Zhang, W., Zeng, X., Huang, Q., Delgado-Baquerizo, M., and Liu, Y.: Climatic seasonality challenges the stability of microbial-driven deep soil carbon accumulation across China, Glob. Change Biol., 29, 4430-4439, https://doi.org/10.1111/gcb.16760, 2023.

Wu, J., Liu, S., Peng, C., Luo, Y., Terrer, C., Yue, C., Peng, S., Li, J., Wang, B., Shangguan, Z., and Deng, L.: Future soil organic carbon stocks in China under climate change, Cell Reports Sustainability., 1(9), 100179. https://doi.org/10.1016/j.crsus.2024.100179, 2024.

Xia, S., Song, Z., Li, Q., Guo, L., Yu, C., Singh, B. P., Fu, X., Chen, C., Wang, Y., and Wang, H.: Distribution, sources, and decomposition of soil organic matter along a salinity gradient in estuarine wetlands characterized by C:N ratio, δ13C-δ15N, and lignin biomarker, Glob. Change Biol., 27, 417-434, https://doi.org/10.1111/gcb.15403, 2021.

Xiao, L., Wang, G., Chang, J., Chen, Y., Guo, X., Mao, X., Wang, M., Zhang, S., Shi, Z., Luo, Y., Cheng, L., Yu, K., Mo, F., and Luo, Z.: Global depth distribution of belowground net primary productivity and its drivers. Glob. Ecol. Biogeogr., 32, 1435–1451. https://doi.org/10.1111/geb.13705, 2023.

Xu, X., Shi, Z., Li, D., Zhou, X., Sherry, R. A., and Luo, Y.: Plant community structure regulates responses of prairie soil respiration to decadal experimental warming, Glob. Change Biol., 21(10), 3846-3853, https://doi.org/10.1111/gcb.12940, 2015.

Xu, X., Thornton, P. E., and Post, W. M.: A global analysis of soil microbial biomass carbon, nitrogen and phosphorus in terrestrial ecosystems, Glob. Ecol. Biogeogr.,

22, 737-749, https://doi.org/10.1111/geb.12029, 2013.

Xu, Y., Zhou, J., Liu, C., Jia, R., Ji, H., Dippold, M. A., Zhao, T., Pavinato, P. S., Peixoxo, L., Yang, Y., Sui, P., Zeng, Z., and Zang, H.: Long–term rotational and perennial cropping benefit soil organic carbon stocks and ecosystem multifunctionality, Ind. Crop. Prod.., 209, 117980. https://doi.org/10.1016/j.indcrop.2023.117980, 2024.

Xu, Y., Xu, X., Li, J., Guo, X., Gong, H., Ouyang, Z., Zhang, L., and Mathijs, E.: Excessive synthetic fertilizers elevate greenhouse gas emissions of smallholder-scale staple grain production in China, J. Cleaner Prod., https://doi.org/10.1016/j.jclepro.2024.128671, 2024.

Yang, Y., Luo, Y., and Finzi, A. C.: Carbon and nitrogen dynamics during forest stand development: a global synthesis, New Phytol., 190, 977-989, https://doi.org/10.1111/j.1469-8137.2011.03645.x, 2011.

Yin, Y., He, K., Chen, Z., Li, Y., Ren, F., Wang, Z., Wang, Y., Gong, H., Zhu, Q., Shen, J., Liu, X., and Cui, Z.: Agricultural green development to coordinate food security and carbon reduction in the context of China's dual carbon goals, Front. Agric. Sci. Eng., 10(2): 262–267, https://doi.org/10.15302/j-fase-2023496, 2023.

Vanden B., A. J., Gregorich, E. G., Angers, D. A., & Stoklas, U. F. Uncertainty analysis of soil organic carbon stock change in Canadian cropland from 1991 to 2001. Glob. Chang. Biol.., 10(7), 983-994. https://doi.org/10.1111/j.1365-2486.2004.00780, 2004.

von Fromm, S. F., Hoyt, A. M., Sierra, C. A., Georgiou, K., Doetterl, S., and Trumbore, S. E.: Controls and relationships of soil organic carbon abundance and persistence vary across pedo-climatic regions, Glob. Change Biol., 30, e17320. https://doi.org/10.1111/gcb.17320, 2024.

Zhao, S., Schmidt, S., Gao, H., Li, T., Chen, X., Hou, Y., Chadwick, D., Tian, J., Dou, Z., Zhang, W., and Zhang, F.: A precision compost strategy aligning composts and application methods with target crops and growth environments can increase global food production, Nat. Food, 3, 741-752, https://doi.org/10.1038/s43016-022-00584-x, 2022.

Zhang, Y., Guo, X., Chen, L., Kuzyakov, Y., Wang, R., Zhang, H., Han, X., Jiang, Y., and Sun, O.: Global pattern of organic carbon in forest soils, Glob. Change Biol.,

30(6): e17386, https://doi.org/10.1111/gcb.17386, 2024.

Zhou, Z., Ren, C., Wang, C., Delgado-Baquerizo, M., Luo, Y., Luo, Z., Du, Z., Zhu, B., Yang, Y., Jiao, S., Zhao, F., Cai, A., Yang, G., and Wei, G.: Global turnover of soil mineral-associated and particulate organic carbon, Nat. Commun., 15, 5329, https://doi.org/10.1038/s41586-024-02075-3, 2024.

Zosso, C. U., Ofiti, N. O. E., Torn, M. S., Wiesenberg, G. L. B., and Schmidt, M. W. I.: Rapid loss of complex polymers and pyrogenic carbon in subsoils under whole-soil warming, Nat Geosci., 16, 344-348, https://doi.org/10.1038/s41561-023-01142-1, 2023.